CORA Cork Open Research Archive
Cartlann Taighde Oscailte Chorcaí

Title	Hall-effect mobility for a selection of natural and synthetic 2D semiconductor crystals
Authors	Monaghan, Scott;Gity, Farzan;Duffy, Ray;Mirabelli, Gioele;McCarthy, Melissa;Cherkaoui, Karim;Povey, Ian M.;Nagle, Roger E.;Hurley, Paul K.;Lindemuth, Jeffrey R.;Napolitani, Enrico
Publication date	2017-07-03
Original Citation	Monaghan, S., Gity, F., Duffy, R., Mirabelli, G., McCarthy, M., Cherkaoui, K., Povey, I. M. Nagle, R. E., Hurley, P. K., Lindemuth, J. R. and Napolitani, E. (2017) 'Hall-effect mobility for a selection of natural synthetic 2D semiconductor crystals', 2017 Joint International EUROSOI Workshop and International Conference on Ultimate Integration on Silicon (EUROSOI-ULIS), Athens, Greece, 3-5 April, pp. 27-30. doi: 10.1109/ULIS.2017.7962592
Type of publication	Conference item
Link to publisher's version	http://eurosoi-ulis2017.inn.demokritos.gr/ - 10.1109/ULIS.2017.7962592
Rights	© 2017, IEEE. Personal use of this material is permitted. Permission from IEEE must be obtained for all other uses, in any current or future media, including reprinting/republishing this material for advertising or promotional purposes, creating new collective works, for resale or redistribution to servers or lists, or reuse of any copyrighted component of this work in other works.
Download date	2026-10-07 09:29:16
Item downloaded from	https://hdl.handle.net/10468/13308

University College Cork, Ireland
Coláiste na hOllscoile Corcaigh

Hall-effect Mobility for a Selection of Natural and Synthetic 2D Semiconductor Crystals

Scott Monaghan[*], Farzan Gity[¥], Ray Duffy, Gioele Mirabelli, Melissa McCarthy, Karim Cherkaoui, Ian M. Povey, Roger E. Nagle and Paul K. Hurley
Tyndall National Institute, University College Cork, Lee Maltings, Cork, IRELAND

Jeffrey R. Lindemuth
LakeShore Cryotronics, Inc., 575 McCorkle Blvd., Westerville, Ohio 43082-8888, USA

Enrico Napolitani
Dipartimento di Fisica e Astronomia, Università di Padova and CNR-IMM MATIS, Via Marzolo 8, I-35131 Padova, ITALY

[¥]Presenting author: farzan.gity@tyndall.ie; [*]Corresponding author: scott.monaghan@ucc.ie (scott.monaghan@tyndall.ie)

***Abstract*—We present a DC-AC Hall-effect analysis on transition-metal-dichalcogenides comprising natural crystals of molybdenum disulfide and tungsten diselenide; and synthetic crystals of hafnium diselenide, molybdenum ditelluride, molybdenum diselenide and niobium-doped molybdenum disulfide. We observe a wide range of Hall mobility and carrier concentration values with either a net electron or hole carrier type. The synthetic niobium-doped molybdenum disulfide crystal exhibits a net hole carrier type and a carrier concentration approximately two orders of magnitude higher than a non-intentionally doped natural molybdenum disulfide crystal, with an equivalent reduction in Hall mobility. This synthetic niobium-doped molybdenum disulfide crystal also shows a significantly reduced resistivity when compared to the other crystals. Secondary ion mass spectrometry shows higher counts of niobium in the intentionally-doped synthetic niobium-molybdenum disulfide crystal, in addition to various other high contamination counts in both the natural and synthetic molybdenum disulfide crystals, correlating well with the significant range of high resistivity observed. Compared to silicon, the resistivity in these contaminated TMD materials reduces less rapidly with increasing equivalent carrier concentration levels, and the resistivity is higher in magnitude by a factor of approximately 4-10 when compared to silicon, which in turn reduces the achievable Hall mobility by at least a similar factor. It is therefore suggested that more controlled growth methods of TMD materials which lead to significantly reduced contamination elements and levels, with improved stoichiometry, could potentially provide a significant increase in Hall mobility assuming no change in carrier properties.**

Keywords*—DC Hall; AC Hall; 2D materials; transition-metal-dichalcogenides; TMDs; crystals; transition metals; chalcogens; resistivity; mobility; semiconductor; secondary ion mass spectrometry (SIMS).

I. INTRODUCTION

One class of material which demonstrates considerable promise as the active semiconductor layer for improved energy efficiency in nanoelectronics, optoelectronics and sensors are transition-metal-dichalcogenides (TMDs), or otherwise known as 2D materials, which have a range of energy gaps that span from semi-metals through to wide band gap semiconductors and as a consequence open up a range of potential applications including those in tunnel FETs, flexible electronics, photovoltaics, and the production of solar fuels using photoelectrochemical cells.

While some progress has already been made in fabricating and characterizing 2D material devices, the control and understanding of what influences carrier and resistance properties in TMD material devices remains at an early stage of research and development [1].

II. EXPERIMENT

Eight natural and synthetic TMD material crystals, as shown in Figure 1 (details in [2]), were received from a commercial supplier and mechanically cleaved to obtain different approximate thicknesses for forming Van der Pauw structures with various contact metals (In, Ag, Ni/Au, and Au). Approximate squares are formed with side length (L), where 0.6cm≤L≤1cm, with the deliberate exception of **S3** which is measured firstly with an irregular shape (**S3a**) and again after forming an approximate square shape (**S3b**) in order to quantify the changing effect on the solution to the Van der Pauw equation (and on the resulting 4-point resistivity), as well as on the Hall carrier properties.

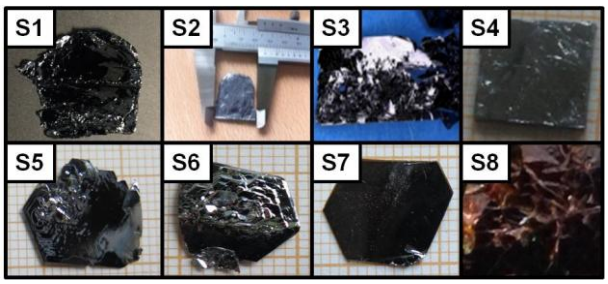

Figure 1: The bulk crystals that sourced **S1**-**S8** of this work (details in [2]): **S1** MoS_2, **S2** MoS_2, **S3** Nb-MoS_2, **S4** MoS_2, **S5** $MoSe_2$, **S6** $MoTe_2$, **S7** WSe_2, and **S8** $HfSe_2$. All sample areas are macroscale for Hall testing.

Room temperature Hall-effect measurements are performed with a LakeShore Model 8404 Hall-Effect Measurement System with DC and AC magnetic fields of ±1.7T (DC) and ~1.2T RMS (AC, 100mHz), respectively. The Hall system uses all combined optimum methods available to calibrate and remove error components [3]. Hall mobility is extracted from the measured Hall voltage and the measured 4-point resistivity for the particular excitation current and magnetic field applied (Hall factor set to unity). Sheet carrier concentration is extracted likewise from the Hall voltage. Tests have been carried out to confirm that no inversion layer formation is contributing to the Hall measurement results (not shown).

Secondary Ion Mass Spectrometry (SIMS) chemical analysis is performed on the natural MoS_2 crystal **S1** and on the synthetic crystal **S3** (Nb-doped MoS_2). Two different primary beams, O_2^+ or Cs^+, where used with a Cameca IMS-4f instrument while collecting positive or negative secondary ions, respectively, in the whole mass range of 1*u*-210*u*. For quantitative analysis, SIMS requires suitable standards that were not available for MoS_2. However, the technique provides useful information on a relative basis by comparing yields collected in different samples.

III. Results and Discussion

A results summary of the DC-AC Hall-effect analysis on samples **S1**-**S8** is provided in Table I. The first observation is that there is good agreement in the extracted properties between the DC and AC Hall-effect methods, and since the AC method is generally efficient at removing error components with a lock-in amplifier, these AC Hall properties are more accurate than the DC extractions [3]. It is observed that all Se-based and Te-based samples (**S5**-**S8**) appear *n*-type (electron shells 4 and 5, respectively, that include *d*-orbitals), whereas most S-based samples (**S1**-**S3**) appear *p*-type (electron shell 3 with no *d*-orbitals, similarly configured to oxygen of electron shell 2), with the exception of the natural *n*-type **S4** sample with a much lower relative carrier concentration and a high mobility.

TABLE I: HALL-EFFECT PROPERTIES FOR THE **S1**-**S8** CRYSTALS.

Material (ID used)	B Field Type	Carrier Type	Hall Mobility (cm^2/V.s)	Resistivity (Ω.cm)	Carrier Conc. (cm^{-3})
MoS_2 (S1)	DC	P	4.571	18.66	$7.318x10^{16}$
MoS_2 (S1)	AC	P	4.442	18.37	$7.647x10^{16}$
MoS_2 (S2)	DC	P	171.3	0.30	$1.056x10^{17}$
MoS_2 (S2)	AC	P	170.9	0.30	$1.059x10^{17}$
Nb-MoS_2 (S3a)	DC	P	6.204	0.014	$7.427x10^{19}$
Nb-MoS_2 (S3a)	AC	P	6.189	0.014	$7.445x10^{19}$
Nb-MoS_2 (S3b)	DC	P	7.962	0.019	$4.068x10^{19}$
Nb-MoS_2 (S3b)	AC	P	7.551	0.019	$4.296x10^{19}$
MoS_2 (S4)	DC	N	124.8	10.71	$4.666x10^{15}$
MoS_2 (S4)	AC	N	113.9	10.69	$5.127x10^{15}$
$MoSe_2$ (S5)	DC	N	103.1	11.67	$5.187x10^{15}$
$MoSe_2$ (S5)	AC	N	105.6	11.72	$5.045x10^{15}$
$MoTe_2$ (S6)	DC	N	61.10	0.359	$2.844x10^{17}$
$MoTe_2$ (S6)	AC	N	62.09	0.351	$2.866x10^{17}$
WSe_2 (S7)	DC	N	142.8	9.576	$4.565x10^{15}$
WSe_2 (S7)	AC	N	130.5	9.672	$4.944x10^{15}$
$HfSe_2$ (S8)	DC	N	7.767	0.18	$4.471x10^{18}$
$HfSe_2$ (S8)	AC	N	7.422	0.18	$4.680x10^{18}$

While in general a wide range of Hall mobility, resistivity and carrier concentration values are observed, it is noticeable that the Nb-doped MoS_2 crystal **S3** has a much lower resistivity and a much higher carrier concentration compared to all the other 2D crystals. It is instructive to plot the Hall mobility versus the sheet carrier concentration from Table I, and this is shown in Figure 2(a). We also plot the Hall mobility versus the carrier concentration in Figure 2(b). Apart from the unusually high resistive sample **S1** discussed later, we observe very similar best fit trends to the **S2**-**S8** data in both plots, confirming that the dominant carriers are distributed homogeneously in the crystals, each with different thicknesses in the ~130µm-765µm range.

The Figure 2 trends are not overly dissimilar to the drift mobility versus *n*-type and *p*-type impurity concentrations for Si and GaAs in Ref. [4], p.29. Importantly, MoS_2 is observed to potentially exhibit a net *p*-type behavior with a hole mobility as high as ~171 cm^2/V-s.

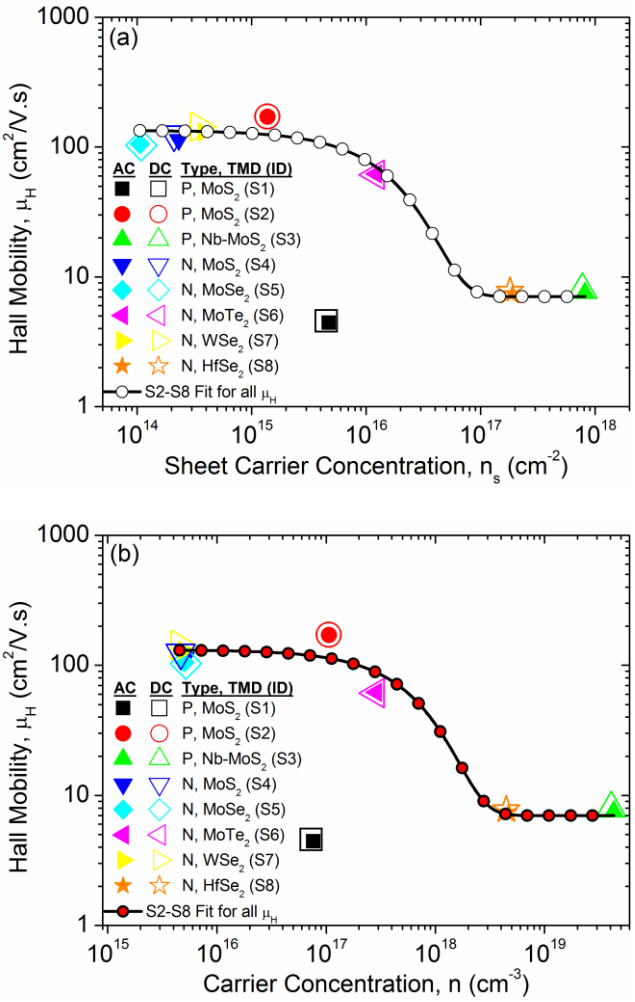

Figure 2: DC-AC Hall mobility versus (a) sheet carrier concentration and (b) carrier concentration. Best non-linear curve fit lines to crystals **S2**-**S8** (**S1** is excluded from the best fit exercise as it is abnormally too resistive). Note that the *y*-axes of the log-log plots (a) and (b) have the same Hall mobility scale to assist in comparing behavior.

Figure 3 reports the SIMS yields of the detected impurities in samples **S1** and **S3**. A large range of (unintentional) impurities are present in both the natural and synthetic MoS_2, consistent with reports via inductively coupled plasma mass spectrometry analysis [5], and likely limiting the achievable mobility as expected by theory [6].

Niobium can clearly be seen in the intentionally-doped synthetically-grown **S3** sample with a yield ~450 higher than in the natural **S1** sample, which is in good agreement with the measured *p*-type carrier concentration levels for **S3**, even if we cannot exclude that the detected Sb is not contributing to the observed *p*-type doping in the natural **S1** sample. Na and Cr are present in the synthetically-grown

sample but, as those elements are expected with high sensitivity, their concentrations are presumed moderate.

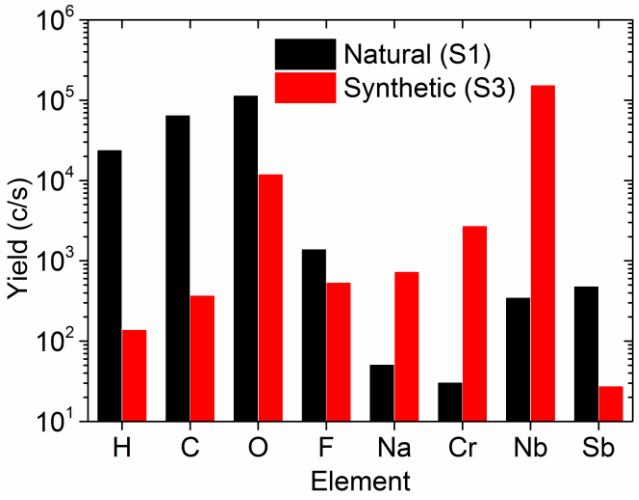

Figure 3: SIMS raw yields of impurities in natural MoS_2 (**S1**) and in synthetically-grown Nb-doped MoS_2 (**S3**). H, C, O, F and Sb were collected as negative ions while sputtering with a Cs^+ beam. Na, Cr and Nb were collected as positive ions while sputtering with a O_2^+ beam. No direct same-sample yield comparisons are given, only between different samples.

H, C, and O are observed in the natural **S1** sample with significantly higher yields than in the synthetically-grown **S3** sample, which we believe are remarkably high and leads to significant increases in the yields of other secondary molecular ions (not shown) formed with such species (e.g. MoC^-, MgO^-, etc.). We speculate that the presence of such impurities at anomalously high concentrations may contribute to the much larger resistance observed in **S1**.

We also observe a possible correlation between the *p*-type behavior of **S1**-**S3** from Table I, the very high oxygen content of **S1** from Figure 3, and the known preference for higher oxidized Molybdenum (in a tri-oxide form) to give *p*-type behavior, as observed in solar cell research and in sub-stoichiometric form for MoO_x-MoS_2 MOSFETs [7].

The question now raised is how is the resistivity behaving in the presence of these high contamination levels with respect to carrier concentration, considering the Hall mobility is an inverse function of the resistivity (ρ), the carrier concentration (n), and the elementary electronic charge (e = 1.60218 x 10^{-19} C), namely $\mu_H = 1/(\rho.n.e)$? To assess the behavior, it is constructive to compare it to the known equivalent behavior for silicon at 300K (see Ref. [4], p.32).

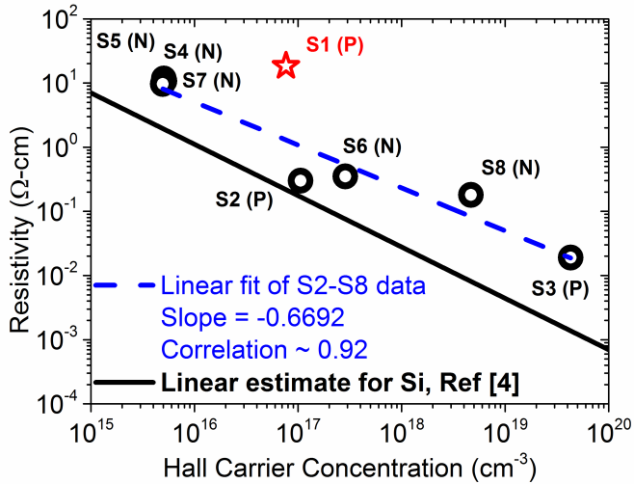

Figure 4: A log-log scatter plot of resistivity versus carrier concentration for **S1**-**S8** of this work, with the data points labelled. **S1** is included but excluded from the behavioral analysis for the reasons discussed earlier. A linear fit to the log-log data for **S2**-**S8** is shown (dashed line, blue, slope = -0.6692, and correlation ~ 0.92), and an approximate representation (estimating both *n*-type and *p*-type in one) of the equivalent behavior for silicon at 300K from [4] is also shown (solid line, black, slope = -0.8).

Figure 4 is a log-log scatter plot of resistivity versus carrier concentration for **S1**-**S8** of this work, with the data points labelled. **S1** is included but excluded from the behavioral analysis for the reasons discussed earlier. A linear fit to the log-log data for **S2**-**S8** is shown (dashed line, blue), and an approximate representation (estimating both *n*-type and *p*-type in one) of the equivalent behavior for silicon at 300K from [4] is also shown (solid line, black).

We firstly observed that the linear fit of the **S2**-**S8** data has a linear fit correlation of only ~0.92, and it appears the greatest deviations occur around the mid-levels of carrier concentration, with higher magnitude resistivity deviations above mid-level carrier concentration, and lower magnitude resistivity deviations below mid-level carrier concentration. Nevertheless, the linear fit is a reasonable representation of the **S2**-**S8** behavior.

The slope of the linear data fit is -0.6692, which is less steep than the estimated black line representation for silicon from Ref. [4] of -0.8, which gives an important indicator that we have less of a reduction in resistivity as we increase the carrier concentration in these TMD materials.

Another important observation when comparing the linear fit to the data and the estimated black line representation for silicon from Ref. [4] is that the resistivity magnitude for the TMD materials is ~4x higher than for silicon at low ~5 x 10^{15} cm^{-3} carrier concentration levels and ~10x higher than for silicon at high ~5 x 10^{19} cm^{-3} carrier concentration levels. Therefore, it can be clearly deduced that this comparatively higher magnitude and shallower slope for the resistivity versus carrier concentration for the TMD materials when compared to silicon will reduce the Hall mobility by a factor of ~4-10 depending on carrier concentration when compared to silicon.

If we assume that this Hall mobility reduction factor range of ~4-10 is resulting from the observed contaminants in these TMD materials, and that purification processes can be developed to improve the long range resistivity and stoichiometry of the TMD materials towards (or even beyond) that observed in silicon without changing the Hall carrier concentration properties, then it may become possible in the future to remove the observed Hall mobility reduction factor range of ~4-10 in comparison to silicon and thus improve on our observed Hall mobility range given in Table I and Figure 2 to levels up to or beyond ~450 $cm^2/V.s$ at low ~5 x 10^{15} cm^{-3} carrier concentration, and ~75 $cm^2/V.s$ at higher ~5 x 10^{19} cm^{-3} carrier concentration for highly pure, stoichiometric, TMD materials.

IV. Conclusions

We present a DC-AC Hall-effect analysis on transition-metal-dichalcogenide 2D materials comprising natural crystals of MoS_2 and WSe_2, and synthetic crystals of $HfSe_2$, $MoTe_2$, $MoSe_2$ and Nb-doped MoS_2, which have potential applications in tunnel FETs, nanoelectronics, optical and sensing devices.

We observe Hall mobility (carrier concentration) values from ~7.6 cm^2/V.s (4.3×10^{19} cm^{-3}, *p*-type) for a synthetic Nb-doped MoS_2 crystal to 171.3 cm^2/V.s (1.1×10^{17} cm^{-3}, *p*-type) for a non-intentionally doped natural MoS_2 crystal. Hence, the Nb-doped MoS_2 synthetic crystal exhibits a net *p*-type carrier type and a carrier concentration approximately two orders of magnitude higher than a non-intentionally doped MoS_2 natural crystal, with an equivalent drop in Hall mobility. The Nb-MoS_2 crystal also shows a significantly reduced resistivity when compared to the other crystals. The relatively high hole mobility observed in MoS_2 (~171 cm^2/V-s) is of particular note, as it points to the possibility of MoS_2 as a single 2D material solution for CMOS based circuits.

Secondary ion mass spectrometry shows higher counts of Nb for an intentionally-doped *p*-type synthetic MoS_2 crystal, in addition to various other high contamination counts in both the natural and synthetic MoS_2, correlating well with the significant range of resistivity and suggests that higher mobility values may be achievable in 2D semiconductors with higher material purity levels.

Assessing this point electrically in comparison to silicon, the resistivity in these contaminated TMD materials reduces less rapidly with increasing equivalent carrier concentration levels, and the resistivity is higher in magnitude by a factor of ~4-10 compared to silicon, which in turn reduces the achievable Hall mobility by at least a similar reduction factor if we assume carrier concentration levels will remain unchanged in equivalent TMD materials grown by alternative controlled methods to achieve good stoichiometry and high purity levels.

It is therefore suggested that such controlled growth methods of TMD materials which lead to significantly reduced contamination elements/levels, with improved stoichiometry, could potentially provide a significant increase in Hall mobility assuming no change in carrier properties.

Finally, these results also suggest that in general terms intentionally doping 2D materials is feasible and can have a significant effect on the electrical properties.

ACKNOWLEDGMENT

We acknowledge Science Foundation Ireland via the US-Ireland R&D Partnership Program, SFI/13/US/I2862 (UNITE). The Hall system was financially supported by Science Foundation Ireland's National Access Program (NAP277) grant number SFI/04/CE/I590a7. The work was also partially supported by the HEA's 5th PRTLI program.

REFERENCES

[1] Z. Lin *et al.*, *2D Mater*. **3**, 042001 (2016)

[2] **S1** (t~615um): Natural MoS_2 (CAS: 1317-33-5, Source A) supplied by HQ Graphene, Groningen, the Netherlands (HQG); **S2** (t~130um): Natural MoS_2 (CAS: 1317-33-5; Source B, HQG); **S3** (t~190um): Synthetically-grown Niobium (Nb) doped MoS_2 (CAS: 1317-33-5, HQG); **S4** (t~450um): Natural MoS_2 (CAS: 1317-33-5; Source C, HQG); **S5** (t~210um): Synthetic $MoSe_2$ (CAS: 12058-18-3, HQG); **S6** (t~425um): Synthetic $MoTe_2$ (CAS: 12058-20-7, HQG); **S7** (t~765um): Natural WSe_2 (CAS: 12067-46-8, HQG); and **S8** (t~405um): Synthetic $HfSe_2$ (CAS: 12162-21-9, HQG)

[3] J. Lindemuth and S. -I. Mizuta, *Thin Film Solar Technology III*, *Proc. of SPIE* **8110**, 81100I (2011)

[4] S. M. Sze, K. K. Ng, *Physics of Semiconductor Devices*, 3rd Ed. (2007), John Wiley & Sons Inc., New Jersey, USA

[5] R. Addou *et al.*, *ACS Nano* **9** (9), 9124 (2015)

[6] N. Ma, D. Jena, *Phys. Rev. X* **4**, 011043 (2014)

[7] S. Chuang *et al.*, *ACS Nano Lett.* **14** (3), 1337 (2014)